Chemistry–A European Journal
Research Article
doi.org/10.1002/chem.202302590
Chemistry Europe
European Chemical Societies Publishing
www.chemeurj.org

Reductive Release from a Hybrid PKS-NRPS during the Biosynthesis of Pyrichalasin H

Henrike Heinemann,[a] Haili Zhang,[a] and Russell J. Cox*[a]

Three central steps during the biosynthesis of cytochalasan precursors, including reductive release, Knoevenagel cyclisation and Diels Alder cyclisation are not yet understood at a detailed molecular level. In this work we investigated the reductive release step catalysed by a hybrid polyketide synthase non-ribosomal peptide synthetase (PKS-NRPS) from the pyrichalasin H pathway. Synthetic thiolesters were used as substrate mimics for in vitro studies with the isolated reduction (R) and holo-thiolation (T) domains of the PKS-NRPS hybrid PyiS. These assays demonstrate that the PyiS R-domain mainly catalyses an NADPH-dependent reductive release of an aldehyde intermediate that quickly undergoes spontaneous Knoevenagel cyclisation. The R-domain can only process substrates that are covalently bound to the phosphopantetheine thiol of the upstream T-domain, but it shows little selectivity for the polyketide.

Introduction

Cytochalasans, such as the phytotoxin pyrichalasin H **1** from the fungus *Pyricularia grisea*, are a structurally diverse family of fungal secondary metabolites with broad biological activities such as anticancer, antibacterial and antiviral agents.[1] The main effect of cytochalasans is the inhibition of actin polymerisation.[2] Cytochalasans are biosynthesised by hybrid polyketide synthase non-ribosomal peptide synthetases (PKS-NRPS) that build a specific polyketide, attached as an amide to the nitrogen of an amino acid. In the case of **1** this is *O*-methyl tyrosine **3**. The amino acid is, in turn, bound as a thiolester to the phosphopantetheine (PP) prosthetic group of a thiolation (T) domain (**4**, Scheme 1A).[3] Immediately downstream of the T-domain is a putative reductive (R) release domain (Scheme 1).

Biosynthetic gene clusters (BGC) involved in the biosynthesis of cytochalasans are well-known. For example, in the case of pyrichalasin H **1** the *pyi* BGC contains a core set of genes encoding the PKS-NRPS itself (PyiS), a *trans*-ER (PyiC) required for correct reduction and programming by the PKS, a Diels-Alderase (DA, PyiF) and an α,β-hydrolase (PyiE) likely involved in formation of **5**.[4,5] In addition, the *pyi* BGC also contains: tailoring genes *pyiBDGH*; *pyiA* that encodes an *O*-methyltransferase; *pyiR* that encodes a pathway-specific transcription factor; and *pyiT* encoding a transporter (Scheme 1B).[6,7] Biosynthetic steps including the synthesis of **3**, and tailoring steps

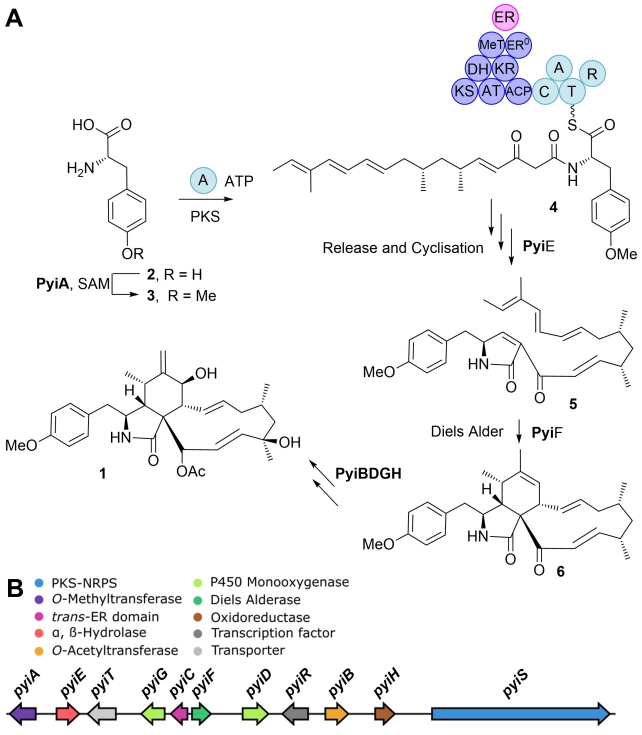

Scheme 1. Proposed biosynthesis of pyrichalasin H **1**. **A**, the proposed biosynthetic route towards pyrichalasin H **1**. **B**, Biosynthetic gene cluster responsible for pyrichalasin H production in *P. grisea*.

catalysed by PyiBDGH are well-understood in vivo.[6] However, the central steps including the proposed release of the enzyme-bound thiolester **4** from PyiS, the subsequent cyclisation step towards the pyrrolinone **5**, and the Diels-Alder reaction forming the cytochalasan core **6**, are not yet understood at a detailed molecular level.

Evidence for PyiE being involved in formation of **5**, and PyiF in the Diels-Alder cyclisation was gained in vivo in previous gene knockout studies.[4,5] However, the intermediate(s) between **4** and **6** have not been directly observed in vivo or

[a] H. Heinemann, Dr. H. Zhang, Prof. Dr. R. J. Cox
Institute for Organic Chemistry and BMWZ
Leibniz Universität Hannover
Schneiderberg 38, 30167 Hannover (Germany)
E-mail: russell.cox@oci.uni-hannover.de

Supporting information for this article is available on the WWW under https://doi.org/10.1002/chem.202302590

in vitro. In principle formation of the pyrrolone **5** could be achieved by three different routes: via Dieckmann cyclisation to tetramic acid **7**, followed by reduction and dehydration; by two-electron reductive release of the aldehyde intermediate **8**, followed by Knoevenagel cyclization; or via four-electron reduction to an alcohol intermediate **9** and subsequent oxidation and cyclisation (Scheme 2A).[3]

R-domains located at the C-termini of PKS and NRPS systems are known to be capable of performing these three different reactions (Scheme 2B).[8,9] For example, enzyme catalysed (non-redox) Dieckmann cyclisations are known to form acyl tetramic acids such as **10**. These domains are named R*-domains or Dieckmann cyclases (DKC)[10] and are exemplified in the case of the cyclopiazonic acid PKS-NRPS CpaS.[10,11,12]

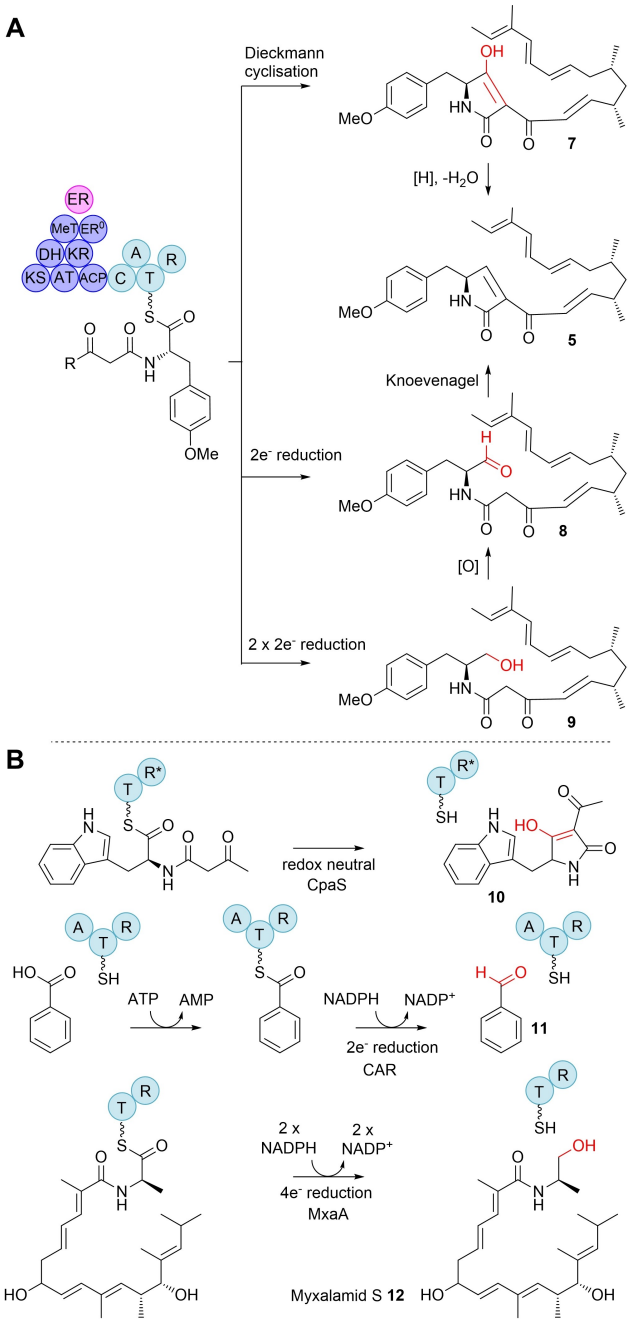

Scheme 2. A, Alternative proposed routes towards pyrrolinone intermediate **5** via Dieckmann cyclisation or four-electron reduction during the biosynthesis of pyrichalasin H **1**; **B**, Known activities of N-terminal R- and R*-domains.

Remarkably, R*- and R-domains share high sequence homology, despite the fact that R*-domains catalyse redox-neutral reactions. On the other hand, R-domains can catalyse an NADPH-dependent reductive release of the T-domain bound thiolester, releasing an aldehyde. Bacterial carboxylic acid reductases (CAR),[13] for example, can convert benzoic acid to benzaldehyde **11** in a two-step process that involves initial ATP-dependent adenylation (A-domain), attachment to the phosphopantetheine (PP) thiol of the T-domain as a thiolester, and final two-electron reduction using NADPH.[14,15] Four-electron reduction to an alcohol has also been observed in the case of the NRPS MxaA that forms myxalamid S **12** (Scheme 2B).[16,17,18] Heterologous expression of cytochalasan PKS-NRPS systems such as those involved in ACE1[5] and cytochalasin E[19] construction in *Aspergillus oryzae* afford the corresponding primary alcohols analogous to **9**, raising the possibility that cytochalasan R-domains could also function by a double reduction. However, such alcohols were not detected in heterologous expression studies of the aspochalasin cluster in *Aspergillus nidulans*. Instead, shunts putatively derived from the pyrrolone intermediate analogous to **5**, were detected.[20]

R and R*-domains belong to the family of short-chain dehydrogenases (SDR). While some bacterial systems (e.g., CAR) have been studied in detail at structural and biochemical levels,[13] fungal systems, and specifically reductive release systems from PKS-NRPS hybrid synthetases have received little attention. Since there is only ca. 20% sequence identity between the CAR TR-didomain and that of PyiS, questions remain regarding the substrate selectivity of the fungal TR-didomains, and whether they function as Dieckmann cyclases, two-electron, or four-electron reductases. We therefore aimed to elucidate the release process and identify the resulting intermediate(s) from the PyiS PKS-NRPS in vitro.

Results

To elucidate the catalytic capacity of the purified PyiS R-domain in vitro, substrate analogues were synthesised. The ideal substrate would be the proposed intermediate **4** (Scheme 1). However, in earlier work with related compounds, the hydrophobicity of the full polyketide, and reactivity of the triene of **4**, had blocked development of in vitro assays.[5] We therefore truncated the polyketide to: an *N*-acetoacetyl group (C_4) that bears the key β-ketone (e.g., **16**); and a simple *N*-acetate (C_2) that lacks this moiety (e.g., **15**). These compounds were synthesised, and in chemical or chemoenzymatic processes attached to backbones mimicking the native PP (Scheme 3). Thus, by using either acetic anhydride **13**, or 2,2,6-trimethyl-4*H*-1,3-dioxin-4-one (TMD) **14**, *O*-methyl tyrosine **3** was converted into amides **15** and **16**, respectively (Scheme 3A). The resulting carboxylic acids were coupled with either *N*-acetylcysteamine **18**, to give the SNAC derivatives **19** and **20**, or pantetheine

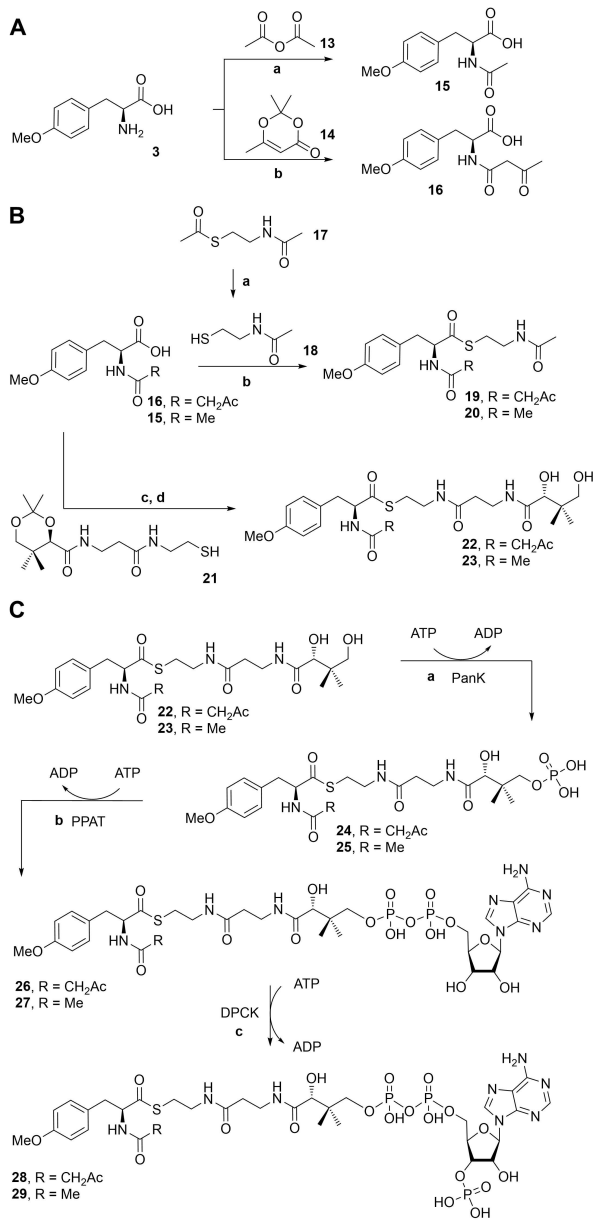

Scheme 3. Chemical and chemoenzymatic synthesis of substrate analogues. Reagents and conditions: **A**, **a**, acetic anhydride **13**, H_2O, NaOH to pH 9–11, 0 °C, then HCl to pH 1, 0 °C; **b**, K_2CO_3, TMD **14**, H_2O, 100 °C, then HCl to pH 1; **B**, **a**, NaOH, 2 h; **b**, *N*-acetylcysteamine **18**, EDCI, DMAP, CH_2Cl_2, RT, 4 h; **c**, pantetheine dimethyl ketal **21**, EDCI, DMAP, CH_2Cl_2, RT, 4 h; **d**, CH_3CN, H_2O, $InCl_3$, 3 h, RT; **C**, Enzymatic conversion of pantetheine substrates by: PanK to PP-linked substrates; PPAT to dephospho-CoA-linked substrates; and DPCK to CoA-linked substrates.

dimethyl ketal **21**, resulting in pantetheine derivatives **22** and **23** after deprotection (Scheme 3B). These were, in turn, converted to their respective CoA derivatives **28** and **29** by in vitro treatment with pantothenate kinase (PanK),[21] phosphopantetheine adenylyltransferase (PPAT)[21] and dephosphocoenzyme A kinase (DPCK,[21] Scheme 3C, for details and for ESI-MS traces see Figures S1–S3).[21]

Two *E. coli* protein expression plasmids were constructed, containing coding sequences for PyiS T- and PyiS R-domains. T-domain boundaries were set to 3626–3720 and R-domain boundaries to 3721–4064, in order to include potential linker sequences.[22] The PyiS R-domain was expressed in *E. coli* and purified as a soluble, N-terminal his_6-tagged protein. The PyiS T-domain was not soluble as a stand-alone protein unless expressed as a thioredoxin-fusion protein (TrxA-T, Figures S4 and S5).

Correct folding of *apo*-TrxA-T-domain was demonstrated via in vitro phosphopantetheinylation of the active site serine by the promiscuous pantetheinyltransferase Sfp.[23] ESI-MS analysis of the resulting protein (Scheme 4A) identified a mass shift from 24.777 kDa (calc. 24.775 kDa) to 25.116 kDa (calc. 25.115 kDa) consistent with formation of *holo*-TrxA-T.

Confirmation of correctly folded R-domain was achieved by isothermal titration calorimetry (ITC). A dissociation constant of 70 μM for NADPH was determined, indicating the expected interaction between both partners and correct folding of the PyiS R-domain (ESI, Figure S6). Size exclusion chromatography (SEC) coupled to multi-angle light-scattering (MALS) showed the R-protein to be monomeric (Figure S7).

Initial in vitro assays were conducted with the *N*-acetoacetyl-*O*-methyl tyrosine derived subset of substrates. SNAC-linked substrate **19**, pantetheine **22**, phosphopantetheine **24** and CoA derivative **28** were incubated with the purified PyiS R-domain and NADPH under different conditions (varied reaction time, buffer, presence of *apo* or *holo*-TrxA-T-domain). However, none of these free substrates was processed by the PyiS R-domain as revealed by ESI-MS analysis of assay extracts (Figures S8–S12). In two-hour assays no evidence of Dieckmann cyclisation was observed by LCMS, but the Dieckmann product **30** was observed after 24 h (Figure S8) corresponding to slow spontaneous cyclisation in reaction and control.

A more sophisticated approach was then devised that involved covalent linkage of the *N*-acetoacetyl-*O*-methyl tyrosine moiety to the PP group of the *holo*-PyiS T-domain itself. To achieve this, the pantetheinyltransferase Sfp was used to transfer the *S*-acyl PP to the *apo*-TrxA-PyiS T-domain in vitro using the CoA derivative **28** as substrate.[23] Conversion of *apo*-TrxA-T-domain (24.772 kDa, calc. 24.775 kDa) to acyl-*holo*-TrxA-T-domain (25.372 kDa, calc. 25.376 kDa) was directly monitored and confirmed by ESI-MS (Scheme 4B, Figure S13). The acyl-*holo*-TrxA-T-domain was presented to the PyiS R-domain (40 kDa) in the presence of NADPH, resulting in release of the acyl group from the *holo*-TrxA-T-domain (Scheme 4E). The release was observed directly by ESI-MS as a mass shift from acyl-*holo*-TrxA-T-domain to *holo*-TrxA-T after 2 h. However, in the absence of NADPH and/or functional R-domain, only minor amounts of *holo*-TrxA-T-domain were detected, presumably derived via either slow hydrolysis or Dieckmann cyclisation (Schemes 4C, D).

The small molecule products of the reaction were analysed by LCMS. In reactions lacking R-domain or NADPH, hydrolysis product **16** and Dieckmann product **30** were detected as the only products by comparison to synthetic standards (Schemes 5E, F). 1,3-dihydro-2*H*-pyrrol-2-one **31** was detected (R_T 6.8 min, Scheme 5D) in the presence of R-domain and NADPH, in addition to lower amounts of **16** and **30**. The identity of pyrrolone **31** was confirmed by comparison with a synthetic

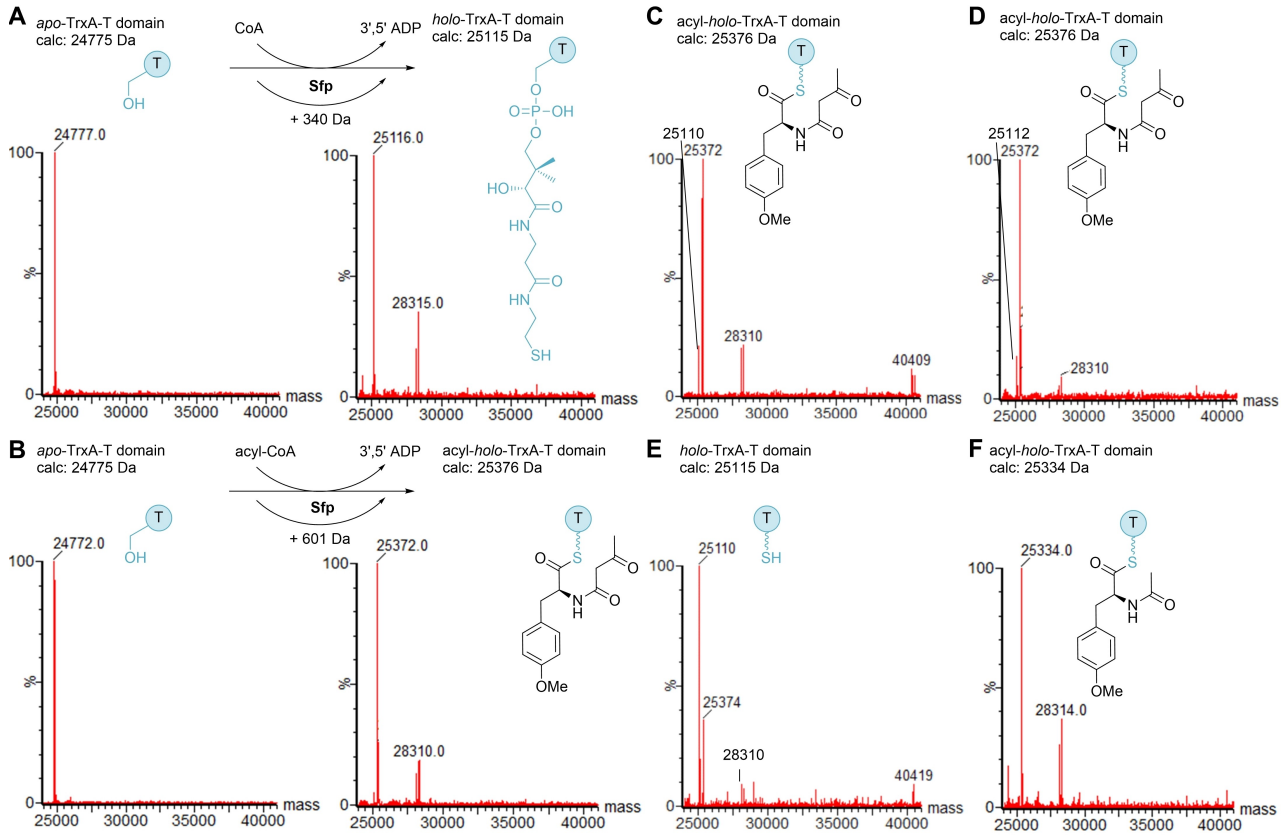

Scheme 4. ESMS analysis of in vitro reductive release studies focussed on protein components. **A**, Sfp-mediated phosphopantetheinylation of *apo*-TrxA-T-domain forming *holo*-TrxA-T-domain using CoA. Left: *Apo*-TrxA-T-domain, right: *Holo*-TrxA-T-domain; **B**, Sfp-mediated formation of acyl-*holo*-TrxA-T-domain using a synthetic CoA derivative **28**. Left: *Apo*-TrxA-T-domain. Right: Acyl-*holo*-TrxA-T-domain; **C**, detection of acyl-*holo*-TrxA-T-domain after incubation with PyiS R-domain without NADPH; Acyl-*holo*-TrxA-T-domain; **D**, detection of acyl-*holo*-TrxA-T-domain after incubation with NADPH and boiled PyiS R-domain; Acyl-*holo*-TrxA-T-domain, **E**, detection of *holo*-TrxA-T-domain after incubation of acyl-*holo*-TrxA-T-domain with NADPH and PyiS R-domain; **F**, Sfp-mediated formation of acyl-*holo*-TrxA-T-domain using synthetic CoA derivative **29**: Acyl-*holo*-TrxA-T-domain. Other proteins detected: His_6-Sfp (calculated mass: 28.133 kDa) with 28.1 kDa and 28.3 kDa (gluconoylated His_6-Sfp); His_6-PyiS R domain (calculated mass: 40.415 kDa) with 40.4 kDa.

standard (Schemes 5B and H, Figure S14–S17). The corresponding alcohol **33** from four-electron reduction was detected under reducing conditions, but at $<4\%$ the level of **31** (ion integration, Figure S18). Aldehyde **32** is already known to cyclise quickly under assay conditions to give the 1,5-dihydro-2*H*-pyrrol-2-one **34** that rapidly tautomerises to 1,3-dihydro-2*H*-pyrrol-2-one **31** (Scheme 5A).[5]

Since the in vitro assay using an *N*-acetoacetyl-*O*-methyl-tyrosine loaded PyiS *holo*-TrxA-T-domain led to detection of the cyclised reductive release product **31**, instead of the aldehyde **32** itself, we sought to directly detect the aldehyde using the *N*-acetyl-*O*-methyl-tyrosine derivative that cannot cyclise. To this end, the CoA derivative of *N*-acetyl-*O*-methyl-tyrosine **29** was loaded onto the PyiS TrxA-T-domain by Sfp. Again, the formation of the correct acyl-*holo*-TrxA-T-domain was confirmed by ESI-MS (Scheme 4F, Figure S19). However, after incubation with NADPH and active PyiS R-domain for 2 h, little *holo*-TrxA-T-domain was observed by ESI-MS (Figure S19). After 4 h around 20% of the acyl-*holo*-TrxA-T-domain was converted into *holo*-TrxA-T-domain. After 4 h around 20% of the acyl-holo-TrxA-T-domain was converted into holo- TrxA-T-domain, showing that reductive release of the *N*-acetyl substrate is less efficient than the *N*-acetoacetyl substrate. In the control reactions lacking functional R-domain or NADPH, only minor amounts of the holo-TrxA-T-domain were observed (Figure S19).

The released aldehyde **36** was identified by comparison to a synthetic standard. The synthesis of **36** (Scheme 6) involved *N*-protection of L-tyrosine **2**, to afford **38**. Double methylation was achieved with MeI under basic conditions. Reduction of methyl ester **39** with $LiAlH_4$ afforded alcohol **40** and basic deprotection gave **41**.[24] Peracetylation with excess acetyl chloride then gave **42**. Selective ester hydrolysis gave **43**[25,26] and then a modified Moffat oxidation gave aldehyde **36**.

The aldehyde **34** rapidly equilibrated with hydrate **44** in water (Figure S20). LCMS analysis of the reaction mixture of the acyl-*holo*-TrxA-T-domain incubated with the PyiS R-domain and NADPH led to the detection of hydrate **42** (Figure S20–21). In control reactions lacking active R-domain or NADPH, neither the aldehyde **36** nor hydrate **44** were detected. However, *N*-acetyl-*O*-methyl tyrosine **15**, from spontaneous hydrolysis, was present in all reactions (Figure S21). Once again, under reducing conditions the double reduction product **43** was observed, but less than 5% the level of **36** based on ion integral (Figures S22–S23).

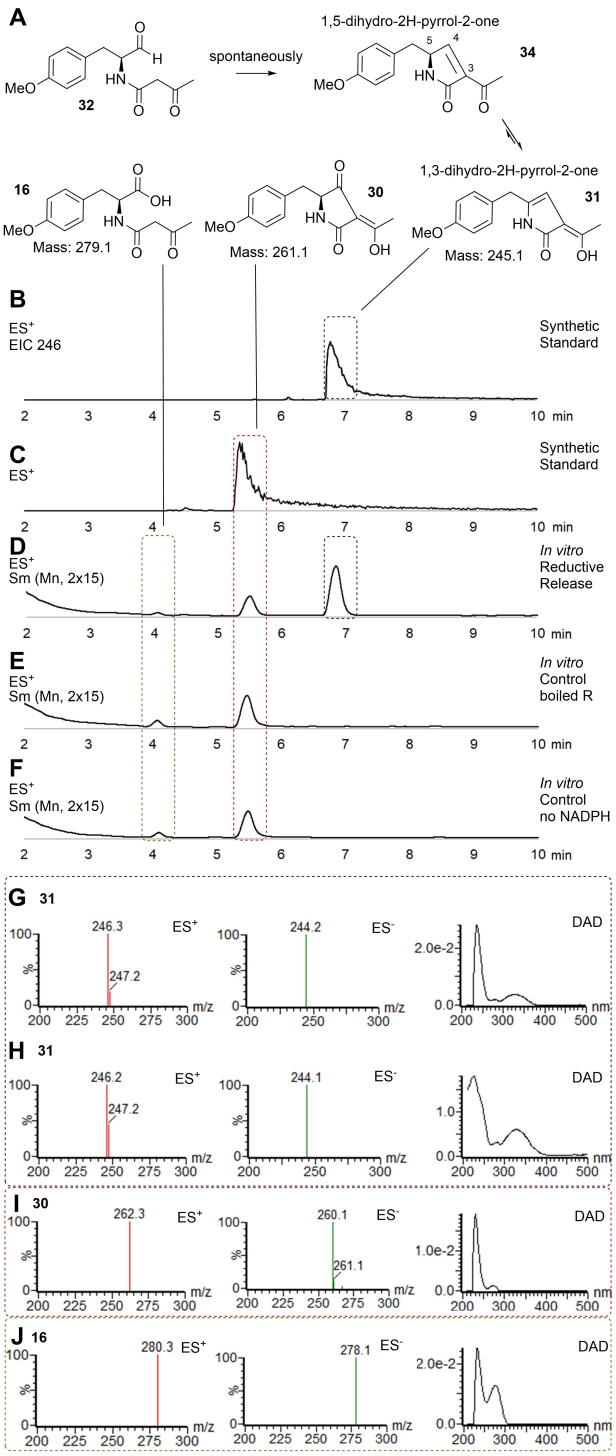

Scheme 5. LCMS analysis of in vitro reductive release studies focussed on small molecule products. **A**, Spontaneous cyclisation and tautomerisation of the aldehyde intermediate **32**; **B**, synthetic standard of 1,3-dihydro-2*H*-pyrrol-2-one **31**; **C**, synthetic standard of tetramate **30**; **D**, in vitro reductive release reaction after incubation of acyl-*holo*-TrxA-T-domain with NADPH and R-domain; **E**, in vitro negative control reaction after incubation of acyl-*holo*-TrxA-T-domain with NADPH and boiled R-domain; **F**, in vitro negative control reaction after incubation of acyl-*holo*-TrxA-T-domain with R-domain without NADPH; **G-J**, ES^+, ES^- and DAD spectra of: **G**, reductive release product **31**; **H**, synthetic standard of 1,3- dihydro-2*H*-pyrrol-2-one **31**; **I**, spontaneous by-product tetramic acid **30**; **J**, spontaneous by-product *N*-acetoacetyl-*O*-methyl tyrosine **16**.

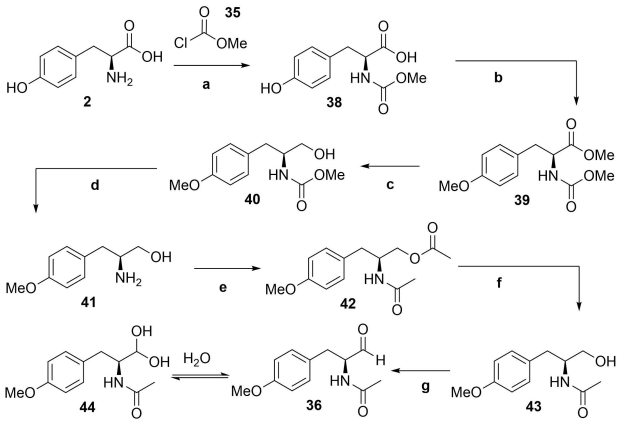

Scheme 6. Synthetic route to aldehyde **36**. Reagents and conditions: **a**, THF, H_2O, $NaHCO_3$, RT, overnight; **b**, MeI, K_2CO_3, DMF, RT, overnight; **c**, $LiAlH_4$, THF, 0 °C, 1 h; **d**, 25 % KOH, MeOH, H_2O, 50 °C, 12 h; **e**, acetyl chloride, CH_2Cl_2, Et_3N, RT, 2 h; **f**, K_2CO_3, MeOH, RT, overnight; **g**, EDC, $Cl_2CHCOOH$, DMSO:Toluene 1:1.

No experimental structural data for fungal R-domains is available. In order to be able to compare our results with previous work in other systems, we generated an unbiased model structure of the PyiS TR-didomain using ColabFold.[27] NADPH was integrated into the model by transfer from the homologous MxaA R-domain (PDB 4U7W)[18] and the PP arm was transferred from the carboxylic acid reductase (CAR) from *Segniliparus rugosus* (PDB 5MSV),[13] onto the T-domain S3673 (see ESI for details of the PyiS TR model building, for example Figures S24–S26). Alignment of the final structural model with available R and TR structures of bacterial and archaeal NRPS results in RMSD values of ~3 Å (Table S7).[28,29] The PyiS TR-didomain forms a V-shaped structure, in which the T-domain and the substrate-binding subdomain rest on the cofactor-binding subdomain (Figure 1A).[18,30] The PyiS T-domain is an α-helical bundle with the serine residue S3673 for PP linkage situated at the beginning of helix-2, as is characteristic for T-domains.[31] The PyiS R domain appears to possess a helix-turn-helix (HTH) interface motif (V4024-V4047), which is conserved in NRPS-R-domains, but is absent in other SDRs (Figure 1A).[30] The nicotinamide cofactor is harbored between the Rossmann fold and the so-called gating loop (see below) in a tunnel. The active site's catalytic tetrad (N3849, T3872, Y3901 and K3905) is conserved with other known structures and appears to form a surface in proximity to the nicotinamide moiety (Figure 1B).[32]

Discussion and Conclusions

Previous in vivo experiments with cytochalasan PKS-NRPS systems have been unable to resolve the precise release mechanism (Scheme 2). Our in vitro work shows conclusively that two-electron NADPH-mediated reduction is the major pathway, releasing an aldehyde (e.g., **32**) that rapidly cyclises to the corresponding pyrrolone (e.g., **31**) in the case of the β-keto substrate analogues derived from **16** (Scheme 4). While slow non-redox Dieckmann cyclisation occurs (e.g., to **30**), and very

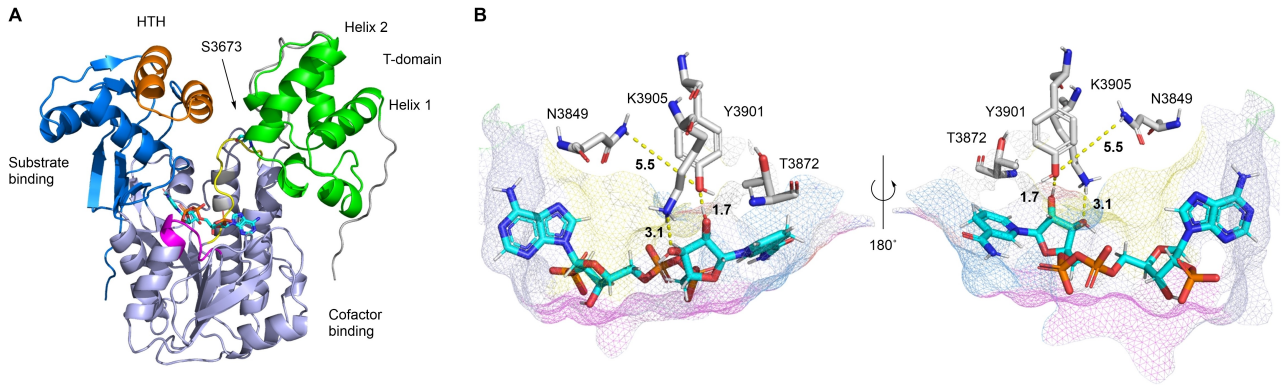

Figure 1. PyiS TR-didomain model. **A**, Overall structure of the TR-didomain showing the T-domain and linkers in green and grey, respectively, the cofactor-binding domain in light blue, the substrate-binding domain in dark blue and the HTH motif in orange. The so-called gating loop is indicated in yellow and the cofactor-binding sequence in magenta. The same colours are used in the multiple sequence alignment (Figure S27). **B**, Detailed view of the cofactor (cyan) bound in the tunnel and catalytic tetrad residues (grey).

slow hydrolysis to **16** is also observed, these reactions are unrelated to the presence or absence of cofactor or protein.

Although the PyiS TR-didomain shows low sequence similarity to the known bacterial TR-systems (*ca* 20% identity to CAR), the developed structural model shows that the PyiS system takes up the same overall structure and aligns to 3.5 Å RMSD with the bacterial CAR system that is a two-electron reductase and 3.0 Å RMSD with the MxaA four-electron TR (20% identity).

The active site tetrad residues of N–S/T–Y–K are conserved in the PyiS R-domain and appear poised to play their known roles (e.g., Figure S25–S27, ESI).[32] It might be expected that loss of these residues could convert a reductase (R) to a cyclase (R*). TR* enzymes are interesting because they have the same overall fold as TR-didomains, but they catalyse a redox-neutral Dieckmann cyclisation. Loss of an active site residue as a reason for loss of reductase activity could be true in the case of the CpaS R*-domain where the key Y is replaced by L,[12] but not in the case of the FsdS R*-domain where N–S–Y–K is present.[11] In the case of the FsdS R*-domain the enzyme does not require cofactor and it might therefore be assumed that R* release is a default reaction in the absence of faster reduction. Liu and Walsh have suggested that R* release could be a default offloading mechanism when reduction does not occur.[12] In the PyiS system, where again the full compliment of active site residues appears to be present, we did observe slow spontaneous release but this was not catalysed by the protein and did not require cofactor. Also, in the case of PyiS, we observed that the R-domain did not accelerate this possible default mode of release over background levels.

This contrasts with previous in vitro assays with R*-domains from the CpaS and fusaridione (FsdS) systems where rapid Dieckmann cyclisation is catalysed.[11,12,33]

One conceivable way in which reduction could be suppressed in favour of R* release would be by blocking the cofactor-binding site. Indeed, in the case of a TR-didomain from a mycobacterial NRPS[34] it was proposed that a loop in the cofactor-binding subdomain, the so called "gating loop", could block the cofactor-binding site in the absence of a fully mature PP-bound substrate.[30,34] In the case of PyiS this does not appear to be the case because we showed that NADPH binds to the isolated R-domain in the absence of the T-domain and PP. This is consistent with observations that in R-domains performing two-electron reductions, NADPH and substrate binding follows a random bi-bi kinetic mechanism.[35]

Moreover, in the case of CpaS, aspartate D3803 was correlated with the Dieckmann cyclisation activity.[12] Our sequence alignment and model show that this residue is conserved in PyiS (D3966) that does not catalyse Dieckmann cyclisation. Thus, the presence or absence of this residue does not appear to control the selectivity of R vs R* release alone, and a more complex mechanism to differentiate R and R* reactions must be in play. Further work will be required to probe this in detail.

The in vitro assays reveal that the PyiS R-domain only reduces T-domain-bound thiolesters. All other possible free substrates were inactive (ESI Figure S8–12). Likewise, assays in which free substrates were incubated with the R-domain and NADPH in the presence of *holo*- or *apo*-T-domain were also catalytically-inactive. Lack of reaction of the free substrates suggests two possible selectivity mechanisms. First, it may be that the active site of the R-domain possesses low affinity for substrates, so that only tethered substrates react fast enough. Alternatively, it may be that binding of the T-domain and its PP is required to set up a conformational change in the R-domain to allow it to bind cofactor and substrate. However, the second possibility seems unlikely given that we observed NADPH binding to the R-domain in the absence of T, and that even in the presence of *apo*- or *holo*-T-domain, non-tethered substrates were not processed.

The diketide β-ketoamide substrate **16** and *N*-acetate **15** are significantly shorter than the true PyiS octaketide substrate **4**, but both are successfully reduced in vitro when attached as thiolesters to the PP of the T-domain, showing that the R-domain possesses little selectivity for the polyketide, consistent with the previous conclusion of low affinity between the substrate and the R-domain active site.

Our previous observations that diverse aminoacyl substrates created by mutasynthesis can be released by the PyiS R-domain also suggest low selectivity for the amino acid component.[36] In other related work, in which the tenellin PKS-NRPS was engineered to vary the chain-length between tetraketides and heptaketides with different methylation patterns, all products were successfully off-loaded by the TENS R*-domain.[37] This observation is also consistent with that in the bacterial CAR system where PP-tethered substrate did not strongly interact with the R-domain active site.[13]

The low substrate-selectivity of the PyiS R-domain is consistent with most observations to-date that indicate that the PKS component in hybrid PKS-NRPS systems controls the polyketide chain-length by failing to extend particular β-keto intermediates.[38] Such stalled β-keto intermediates appear to be passed to the NRPS to be attached to the appropriate amino acid (i.e., A-domain selectivity) prior to reductive release in the case of cytochalasans or Dieckmann release in the case of acyl-tetramic acids.[37] It thus makes sense that the downstream domains such as R do not have high intrinsic selectivity - they reduce the substrates they receive. This also enables evolution of the PKS to produce new structures, without the requirement for co-evolution of the release domain.

The PyiS TR-release domain predominantly reduces once to release aldehydes. Evidence of double reduction was detected, but at only up to 5% of the amount of aldehyde products. This indicates that the aldehydes **32** and **36** can either remain in, or re-enter, the active site while the cofactor is replaced at a low level. Since non-tethered groups are not reduced by the R-domain, it seems likely that the reduced aldehyde lingers in the active site while the cofactor is replaced. In systems that do catalyse double reduction such as the MxaA R-domain, this kinetic mechanism also seems likely, as the MxaA R-domain is also unable to process non-tethered substrates.

Primary alcohols corresponding to **9** have been observed in vivo when some cytochalasin PKS-NRPS are expressed in fungal hosts.[5,19] These alcohols must arise from rapid reduction of the released aldehydes by adventitious enzymes in the host organism, since the TR-didomain does not catalyse double reduction to an appreciable degree.

Collectively, the results of our in vitro studies show that the T-domain bound thiolester intermediate is released in a single two-electron reduction as an aldehyde and fast spontaneous Knoevenagel cyclisation forms the observed pyrrolone intermediate. This is the first detailed evidence for the biosynthetic role of the PKS-NRPS R-domain during the biosynthesis of cytochalasans. Our results highlight the lack of strong hypotheses and experimental evidence regarding the mechanism that controls the selectivity of these systems for Dieckmann, single-reductive or double-reductive release and further detailed structural work will be required to untangle these effects. However, the PyiS R-domain appears to show very low selectivity for its PP-tethered substrate, and its ability to act as an unselective release mechanism will be advantageous for future cytochalasan engineering work. The results of this study also build a platform for further in vitro studies of the chemical steps catalysed by the α,β-hydrolase PyiE[5] and Diels-Alderase PyiF,[4] that follow the reductive release.

Acknowledgements

HH was funded by LUH. DFG Forschergruppe 5170 CytoLabs is also thanked for funding. H.Z. was funded by the China Scholarship Council (CSC 201506200065). Open Access funding enabled and organized by Projekt DEAL.

Conflict of Interests

The authors declare no conflict of interest.

Data Availability Statement

The data that support the findings of this study are openly available in Figshare at 10.6084/m9.figshare.23552250, reference number 1.

Keywords: cytochalasan · non-ribosomal peptide · reductive release · polyketide · SDR

[1] K. Scherlach, D. Boettger, N. Remme, C. Hertweck, *Nat. Prod. Rep.* **2010**, *27*, 869–886.
[2] R. Kretz, L. Wendt, S. Wongkanoun, J. Luangsa-ard, F. Surup, S. Helaly, S. Noumeur, M. Stadler, T. Stradal, *Biomol. Eng.* **2019**, *9*, 73.
[3] E. Skellam, *Nat. Prod. Rep.* **2017**, *34*, 1252–1263.
[4] V. Hantke, E. J. Skellam, R. J. Cox, *Chem. Commun. (Camb.)* **2020**, *56*, 2925–2928.
[5] H. Zhang, V. Hantke, P. Bruhnke, E. J. Skellam, R. J. Cox, *Chem. Eur. J.* **2021**, *27*, 3106–3113.
[6] C. Wang, V. Hantke, R. J. Cox, E. Skellam, *Org. Lett.* **2019**, *21*, 4163–4167.
[7] C. Wang, K. Becker, S. Pfütze, E. Kuhnert, M. Stadler, R. J. Cox, E. Skellam, *Org. Lett.* **2019**, *21*, 8756–8760.
[8] M. Mullowney, R. A. McClure, M. T. Robey, N. L. Kelleher, R. J. Thomson, *Nat. Prod. Rep.* **2018**, *35*, 847–878.
[9] L. Du, L. Lou, *Nat. Prod. Rep.* **2010**, *27*, 255–278.
[10] L. M. Halo, J. W. Marshall, A. A. Yakasai, Z. Song, C. P. Butts, M. P. Crump, M. Heneghan, A. M. Bailey, T. J. Simpson, C. M. Lazarus, R. J. Cox, *ChemBioChem* **2008**, 585–594.
[11] J. W. Sims, E. W. Schmidt, *J. Am. Chem. Soc.* **2008**, *130*, 11149–11155.
[12] X. Liu, C. T. Walsh, *Biochemistry* **2009**, *48*, 8746–8757.
[13] D. Gahloth, M. S. Dunstan, D. Quaglia, E. Klumbys, M. P. Lockhart-Cairns, A. M. Hill, S. R. Derrington, N. S. Scrutton, N. J. Turner, D. Leys, *Nat. Chem. Biol.* **2017**, *13*, 975–981.
[14] D. J. Wilson, C. Shi, A. M. Teitelbaum, A. M. Gulick, C. C. Aldrich, *Biochemistry* **2013**, *52*, 926–937.
[15] K. Koketsu, K. Watanabe, H. Suda, H. Oguri, H. Oikawa, *Nat. Chem. Biol.* **2010**, *6*, 408–410.
[16] A. Chhabra, A. S. Haque, R. K. Pal, A. Goyal, R. Rai, S. Joshi, S. Panjikar, S. Pasha, R. Sankaranarayanan, R. S. Gokhale, *Proc. Natl. Acad. Sci. USA* **2012**, *109*, 5681–5686.
[17] Y. Li, K. J. Weissman, R. Müller, *J. Am. Chem. Soc.* **2008**, *130*, 7554–7555.
[18] J. F. Barajas, R. M. Phelan, A. J. Schaub, J. T. Kliewer, P. J. Kelly, D. R. Jackson, R. Luo, J. D. Keasling, S. C. Tsai, *Chem. Biol.* **2015**, *22*, 1018–1029.
[19] R. Fujii, A. Minami, K. Gomi, H. Oikawa, *Tetrahedron Lett.* **2013**, *54*, 2999–3002.
[20] J.-M. Zhang, X. Liu, Q. Wei, C. Ma, D. Li, Y. Zou, *Nat. Commun.* **2022**, *13*, 225.
[21] I. Nazi, K. P. Koteva, G. D. Wright, *Anal. Biochem.* **2004**, *324*, 100–105.

[22] B. O. Bachmann, J. Ravel, *Methods for In Silico Prediction of Microbial Polyketide and Nonribosomal Peptide Biosynthetic Pathways from DNA Sequence Data in Methods in Enzymology*, Vol. 458 (Eds.: J. N. Abelson, M. I. Simon), **2009**, pp. 181–217.
[23] R. H. Lambalot, A. M. Gehring, R. S. Flugel, P. Zuber, M. LaCelle, M. A. Marahiel, R. Reid, C. Khosla, C. T. Walsh, *Chem. Biol.* **1996**, *3*, 923–936.
[24] M. Ousmer, N. A. Braun, C. Bavoux, M. Perrin, M. A. Ciufolini, *J. Am. Chem. Soc.* **2001**, *123*, 7534–7538.
[25] V. Dambrin, J. Lenoir, J. Schneider, **2003**, WO 2005/058810A1.
[26] Z. Abbas, X. H. Hu, A. Ali, Y. W. Xu, X. P. Hu, *Tetrahedron Lett.* **2020**, *61*, 151860.
[27] M. Mirdita, K. Schütze, Y. Moriwaki, L. Heo, S. Ovchinnikov, M. Steinegger, *Nat. Methods* **2022**, *19*, 679–682.
[28] Z. Li, L. Jaroszewski, M. Iyer, M. Sedova, A. Godzik, *Nucleic Acids Res.* **2020**, *48*, W60-W64.
[29] Y. Ye, A. Godzik, *Bioinformatics* **2003**, *19*, ii246-ii255.
[30] S. Deshpande, E. Altermann, V. Sarojini, J. S. Lott, T. V. Lee, *J. Biol. Chem.* **2021**, *296*, 100432.
[31] T. Weber, R. Baumgartner, C. Renner, M. A. Marahiel, T. A. Holak, *Structure* **2000**, *8*, 407–418.
[32] K. L. Kavanagh, H. Jörnvall, B. Persson, U. Oppermann, *Cell. Mol. Life Sci.* **2008**, *65*, 3895–3906.
[33] W. Xu, X. Cai, M. E. Jung, Y. Tang, *J. Am. Chem. Soc.* **2010**, *132*, 13604–13607.
[34] P. Kinatukara, K. D. Patel, A. S. Haque, R. Singh, R. S. Gokhale, R. Sankaranarayananan, *J. Struct. Biol.* **2016**, *194*, 368–374.
[35] A. S. Haque, K. D. Patel, M. V. Deshmukh, A. Chhabra, R. S. Gokhale, R. Sankaranarayanan, *J. Struct. Biol.* **2014**, *187*, 207–214.
[36] C. Wang, C. Lambert, M. Hauser, A. Deuschmann, C. Zeilinger, K. Rottner, T. E. B. Stradal, M. Stadler, E. J. Skellam, R. J. Cox, *Chem. A Eur. J.* **2020**, *26*, 13578–13583.
[37] X. L. Yang, S. Friedrich, S. Yin, O. Piech, K. Williams, T. J. Simpson, R. J. Cox, *Chem. Sci.* **2019**, *10*, 8478–8489.
[38] R. J. Cox, *Nat. Prod. Rep.* **2022**, *40*, 9–27.

Manuscript received: September 8, 2023
Accepted manuscript online: November 5, 2023
Version of record online: November 27, 2023